

FREQUENTIST FORECASTING IN REGIME-SWITCHING MODELS WITH
EXTENDED HAMILTON FILTER

KENTO OKUYAMA

UNIVERSITY OF TÜBINGEN

TIM FABIAN SCHAFFLAND

UNIVERSITY OF TÜBINGEN, D-FINE GMBH

PASCAL KILIAN

UNIVERSITY OF TÜBINGEN, ROBERT BOSCH GMBH

HOLGER BRANDT

UNIVERSITY OF TÜBINGEN

AUGUSTIN KELAVA

UNIVERSITY OF TÜBINGEN

Correspondence should be sent to Kento Okuyama, Methods Center, University of Tübingen, 72076, Germany.

E-Mail: kento.okuyama@uni-tuebingen.de

FREQUENTIST FORECASTING IN REGIME-SWITCHING MODELS WITH EXTENDED KIM FILTER

Abstract

Psychological change processes, such as university student dropout in math, often exhibit discrete latent state transitions and can be studied using regime-switching models with intensive longitudinal data (ILD). Recently, regime-switching state-space (RSSS) models have been extended to allow for latent variables and their autoregressive effects. Despite this progress, estimation methods for handling both intra-individual changes and inter-individual differences as predictors of regime-switches need further exploration. Specifically, there's a need for frequentist estimation methods in dynamic latent variable frameworks that allow real-time inferences and forecasts of latent or observed variables during ongoing data collection. Building on Chow and Zhang's (2013) extended Kim filter, we introduce a first frequentist filter for RSSS models which allows hidden Markov(-switching) models to depend on both latent within- and between-individual characteristics. As a counterpart of Kelava et al.'s (2022) Bayesian forecasting filter for nonlinear dynamic latent class structural equation models (NDLC-SEM), our proposed method is the first frequentist approach within this general class of models. In an empirical study, the filter is applied to forecast emotions and behavior related to student dropout in math. Parameter recovery and prediction of regime and dynamic latent variables are evaluated through simulation study.

Key words: regime-switching, state-space, forecasting, Kim filter, frequentist

Recently, the increasing availability of intensive longitudinal data (ILD) has been brought about by digital devices such as mobile phones and smartwatches. ILD typically consists of data from several subjects, with around thirty to a hundred repeated measures per subject. The data could take various forms, such as self-report, physiological data, and behavioral, environmental, and geographic data (Trull and Ebner-Priemer, 2014). Parts of such data may be time-invariant, i.e., stable across time points (*inter-individual*; e.g., dispositions, personal traits). Other parts of the data consist of repeated measures whose states are subject to dynamic changes across time within individuals (*intra-individual*; e.g., affective states).

Structural equation model (SEM) has been one of the most important methods in psychometrics. Dynamic SEM (DSEM; Tihomir Asparouhov and Muthén, 2018), which combines SEM and time-series analysis, has been actively studied to investigate the change process in ILD. With increasing number of substantive applications of DSEMs, a number of new ILD methods have been developed (e.g., Kelava and Brandt, 2019).

Many psychological change processes are characterized by *regime-switching*, in which a change process is described by discontinuous transitions from one discrete latent state (i.e., regime) to another at a particular time point (see e.g., Hamaker and Grasman, 2012; Asparouhov et al., 2017). Individuals are allowed to switch between regimes over time. In some cases, it is expected that the transition mostly occurs in a unidirectional manner e.g., from an intention to stay at math lecture to an intention to quit (cf., Rubicon model; Achtziger and Gollwitzer, 2018). In other cases, subjects could repeatedly switch back and forth between two or more states such as the sleep-wake cycle (Ji et al., 2020). Studying such processes on a within-individual level requires a regime-switching model that assumes that each observation comes from one of the distinct distributions, each of which has a unique set of parameters (e.g., mean, variance, autocorrelation).

Since Markov-switching autoregressive (MSAR) models (Hamilton, 1989) were introduced, regime-switching models have mostly gained the interest of econometricians. Kim (1994) generalized this approach to state-space models, which are called regime-switching state-space (RSSS) models. This framework accommodated a wide range of models, including latent variable models and regime-dependent time-series models (Yang and Chow, 2010).

Chow and Zhang (2013) then developed nonlinear RSSS models, whose state-space representation is governed by nonlinear dynamics. The transition between regimes is characterized by a set of transition probabilities that are invariant across individuals over time. Their estimation approach, called the extended Kim filter,

combines the extended Kalman filter and the Hamilton filter to handle the estimation of parameters and latent variables in their nonlinear RSSS models. Filtering (Box et al., 2015) is an important technique as it allows forecasting i.e., real-time inference of unrealized future states and/or events based on available information. Upon each measurement, the prediction is continuously updated, making it suitable for applications which involve real-time monitoring and timely intervention. Upon arrival of the entire time-series observation, their estimation of the latent variables and the regime probabilities could be refined using a smoothing procedure called the extended Kim smoother.

Kelava et al. (2022) addressed forecasting the precursor of student dropout, referred to as the *intention to dropout*, within their regime-switching modeling framework called the nonlinear dynamics latent class structural equation models (NDLC-SEM). Their flexible NDLC-SEM notation accommodates interactions between *intra-individual* factors and *inter-individual* factors in both their regime-switching model and their state-space model. An estimation procedure called the Forward Filtering Backward Sampling (FFBS; West and Harrison, 2006) is implemented as a Bayesian counterpart to the extended Kim filter and extended Kim smoother. Accounting for unobserved heterogeneity in the hidden Markov(-switching) models characterizes the novelty of this approach.

Limitations and scope

These methods have enabled the estimation of diverse nonlinear RSSS models. Notably, they allowed for real-time inferences and forecasts of latent or observed variables based on ongoing collections of ILD. However, there are three limitations in the current state of RSSS models. First, the NDLC-SEM provides a very flexible approach of modeling RSSS models (including intra-individual factors for the prediction of regime membership). It is implemented using a Bayesian estimator which may become computationally very expensive, as it tries to obtain the complete parameter distribution. On the other hand, the goal of the frequentist estimator is to find a point estimate where the likelihood is maximized. Second, existing frequentist approaches do not allow for any forms of intra-individual change, inter-individual differences, and their interaction in transition probabilities. This heavily impacts their use for dynamic modeling of transition probabilities. From an applied perspective, a frequentist estimator that can include dynamic information in updating the state membership is an important next step. Third, the specification of priors is not necessary in the frequentist domain. These models are very complex and theories very often have very vague specification of expected distributions (if at all). There-

fore, the lack of theoretical and empirical anticipation of effects (priors/beliefs) could be a motivation to adapt a frequentist approach.

In this paper, we present a frequentist estimation approach for RSSS models which considers both intra- and inter-individual differences in hidden Markov(-switching) models. The Kim filter is extended for novelty, enabling parameter and latent variable estimation within a frequentist counter-part to the NDLC-SEM framework. Similar to Kelava et al. (2022)'s, our approach accommodates unobserved heterogeneity in the hidden Markov(-switching) models.

The remainder of this article is structured as follows. In the next section we introduce the RSSS modeling framework, followed by a detailed description of the model estimation and the implementation of the extended filter. In an empirical example, we illustrate the approach and its ability to forecast regime membership. Then, we provide further evidence of its performance using a simulation study. We end with a discussion of the strengths and weaknesses of the approach.

Regime-Switching State-Space (RSSS) models

In this section, we provide a brief description of our models that govern the underlying data generating process. The measurement model establishes the relationship between the latent variables and their observed proxies. The structural model depicts the temporal progression of continuous intra-individual latent variables through hidden Markov VAR(1) models, which depend on both inter- and intra-individual variables. The Markov-switching model illustrates the regime-switching mechanisms through transition probabilities. The transition probabilities are described as a function of intra- and inter-individual latent variables as well as their interactions. Lastly, actual regime-switch occurs as a random event based on the transition probabilities.

Measurement model

The measurement model is described by the following linear equations. Dynamic observed variables, which are expressed as $(\mathbf{y}_{1it}|S_{it} = s)$, are conditional on individual i , time t , and a discrete latent state S_{it} . Dynamic latent variables, which are expressed as $(\boldsymbol{\eta}_{1it}|S_{it} = s)$ are also conditional on individual i , time t , and a discrete latent state S_{it} ,

$$(\mathbf{y}_{1it}|S_{it} = s) = \boldsymbol{\Lambda}_{1s}(\boldsymbol{\eta}_{1it}|S_{it} = s) + \boldsymbol{\epsilon}_{1its}, \quad (1)$$

with a conditional vector of uncorrelated residuals $\boldsymbol{\epsilon}_{1its} \sim \mathcal{N}(\mathbf{0}, \mathbf{R}_{1s})$. Let O_1 be the number of time-dependent observed variables and U_1 be the number of time-

dependent latent variables. Λ_{1s} is a factor loading matrix which is dependent on dynamic latent state S_{it} , with a dimension $O_1 \times U_1$. \mathbf{R}_{1s} is an $O_1 \times O_1$ residual covariance matrix which is dependent on a dynamic latent state S_{it} .

Time-invariant observed variables (\mathbf{y}_{2i}) and time-invariant latent variables ($\boldsymbol{\eta}_{2i}$) are dependent on individual i ,

$$\mathbf{y}_{2i} = \Lambda_2 \boldsymbol{\eta}_{2i} + \boldsymbol{\epsilon}_{2i}, \quad (2)$$

where $\boldsymbol{\eta}_{2i} \sim \mathcal{N}(\mathbf{0}, \mathbf{P}_2)$, $\boldsymbol{\epsilon}_{2i} \sim \mathcal{N}(\mathbf{0}, \mathbf{R}_2)$ are vector of residuals. Let O_2 be the number of time-invariant observed variables and U_2 be the number of time- time-invariant latent variables. Λ_2 is a $O_2 \times U_2$ factor loading matrix. \mathbf{P}_2 is a $U_2 \times U_2$ factor covariance matrix and \mathbf{R}_2 is an $O_2 \times O_2$ residual covariance matrix.

Within-level structural model

The within-level structural model is described by the conditional linear equation given a temporal discrete latent state $S_{it} = s$,

$$(\boldsymbol{\eta}_{1it}|S_{it} = s) = \mathbf{b}_{1is} + \mathbf{B}_{3is} \boldsymbol{\eta}_{1i,t-1} + \boldsymbol{\zeta}_{1its}, \quad (3)$$

where $\boldsymbol{\zeta}_{1its} \sim \mathcal{N}(\mathbf{0}, \mathbf{Q}_{1s})$. For person i at time t , $(\boldsymbol{\eta}_{1it}|S_{it} = s)$ represents a $U_1 \times 1$ vector of conditional intra-individual latent scores. \mathbf{b}_{1is} is a $U_1 \times 1$ conditional random intercept vector, \mathbf{B}_{3is} is a $U_1 \times U_1$ matrix of conditional intra-individual VAR(1) effects, and \mathbf{Q}_{1s} is a $U_1 \times U_1$ residual covariance matrix which is dependent on a dynamic latent state S_{it} .

Between-level structural model

For the random intercept vector \mathbf{b}_{1is} and the autoregressive coefficient matrix \mathbf{B}_{3is} , the between-level structural model is specified by two models:

$$\mathbf{b}_{1is} = \mathbf{b}_{1s} + \mathbf{b}_{2s} \boldsymbol{\eta}_{2i} + \boldsymbol{\zeta}_{2i}, \quad (4)$$

$$\mathbf{B}_{3is} = \mathbf{B}_{3s} + \mathbf{B}_{4s} \boldsymbol{\eta}_{2i}, \quad (5)$$

where \mathbf{b}_{1s} is a $U_1 \times 1$ conditional intercept vector, \mathbf{b}_{2s} is a $U_1 \times 1$ vector of conditional inter-individual effects, $\boldsymbol{\zeta}_{2i}$ is a $U_1 \times 1$ vector of random intercepts with $\boldsymbol{\zeta}_{2i} \sim \mathcal{N}(\mathbf{0}, \mathbf{Q}_2)$. \mathbf{Q}_2 is a $U_2 \times U_2$ residual covariance matrices. \mathbf{B}_{3s} is a $U_1 \times U_1$ matrix of conditional intra-individual VAR(1) effects, and \mathbf{B}_{4s} is a $U_1 \times U_1$ matrix of conditional interaction effects.

Markov-switching model

The transition probabilities are characterized using a nonlinear function of the latent variables of the between- and within-level structural models:

$$Pr[S_{it} = 1|S_{i,t-1} = s'] = \sigma(\gamma_{s'1} + \gamma_{s'2}\boldsymbol{\eta}_{2i} + \boldsymbol{\gamma}_{s'3}\boldsymbol{\eta}_{1i,t-1} + \boldsymbol{\gamma}_{s'4}\boldsymbol{\eta}_{1i,t-1}\boldsymbol{\eta}_{2i}), \quad (6)$$

$$Pr[S_{it} = 2|S_{i,t-1} = s'] = 1 - Pr[S_{it} = 1|S_{i,t-1} = s'], \quad (7)$$

where $s, s' \in \{1, 2\}$ indicates the regime membership (e.g., $s = 1$: no dropout intention; $s = 2$: dropout intention). σ represents the sigmoid function i.e., $\sigma(x) = [1 + \exp(-x)]^{-1}$. $\gamma_{s'1}$ is an intercept, $\gamma_{s'2}$ is a scalar coefficient corresponding to the effect of an inter-individual factor, $\boldsymbol{\gamma}_{s'3}$ is a $1 \times U_1$ vector of the effects of intra-individual factors, and $\boldsymbol{\gamma}_{s'4}$ is a $1 \times U_1$ vector of the interaction effects. The underlying regime-switching mechanism is described as a random event from the probability distribution $Pr[S_{it} = s|S_{i,t-1} = s']$.

Parameter Estimation and Forecasting

The proposed parameter estimation procedure is summarized in Algorithm 1. Factor scores of inter-individual latent variables are calculated (step 1). Then, the extended Kim filter, which is composed of the extended Kalman filter, the extended Hamilton filter, and the collapsing process, is used to filter RSSS models (step 2-4). Based on the distributional assumptions, the prediction errors follow a multivariate normal distribution, serving as a basis for parameter updates using an approximated likelihood function¹ (step 5). Given the set of parameter values at time t , the extended Kim filter forecasts the dynamics latent states and the underlying regime memberships for time $t + 1$. The parameter estimates will become available at the end of Algorithm 1; the associated standard errors can be obtained by taking the square root of the diagonal elements of the negative numerical Hessian matrix or its approximation at the estimated point.

The Confirmatory factor analysis (step 1)

The inter-individual latent variables $\boldsymbol{\eta}_{2i}$ are estimated from their observed proxies \mathbf{y}_{2i} using the factor score regression (cf., Skrondal and Laake, 2001). The calculation follows the standard formula:

$$\hat{\boldsymbol{\eta}}_{2i} = \mathbf{F}_2 \mathbf{y}_{2i} \quad (8)$$

¹The likelihood is approximated in the collapsing procedure (Kim and Nelson, 2017) and can be written using the predictive error decomposition function (Schweppe, 1965).

Algorithm 1 Parameter optimization procedure based on the Kim filter

while not converged **do**

1: Confirmatory factor analysis

for $t = 1, \dots, T$ **do**

2: Extended Kalman filter

3: Extended Hamilton filter

4: Collapsing process

end for

5: Parameter update

end while

where \mathbf{F}_2 is the matrix of factor score weights. This matrix is computed based on the current estimates of the measurement model parameters: the factor loading matrix Λ_2 and the residual covariance matrix \mathbf{R}_2 . In the case of Bartlett factor scores (Bartlett, 1937), the formula for \mathbf{F}_2 is:

$$\mathbf{F}_2 = (\Lambda_2^T \mathbf{R}_2^{-1} \Lambda_2)^{-1} \Lambda_2^T \mathbf{R}_2^{-1}. \quad (9)$$

The Bartlett factor scores provide a conditionally unbiased estimate of the factor scores given the observed data.

The extended Kalman filter (step 2)

The original Kalman filter (Kalman, 1960) was proposed as a real-time estimation procedure to estimate the continuous latent variables in a state-space model as well as to predict their future values. The Kalman filter consists of three steps, namely, *prediction*, *measurement*, and *update*.

In step 2.1, a prediction of the augmented latent variables $\boldsymbol{\eta}_{\text{aug},it}$ (which include both the time-dependent $\boldsymbol{\eta}_{1it}$ and the time-invariant ζ_{2i}) is made based on all available information up to the previous time point. The prediction is denoted as $\boldsymbol{\eta}_{\text{aug},it|t-1}$. In step 2.2, the *one-step-ahead-prediction error* is calculated, which is the difference between the time-dependent observed variables \mathbf{y}_{1it} and their prediction $\mathbf{y}_{1it|t-1}$ (derived from $\Lambda_{1s,\text{aug}} \boldsymbol{\eta}_{\text{aug},it|t-1}$). In step 2.3, the prediction of the augmented latent variables $\boldsymbol{\eta}_{\text{aug},it|t}$ is updated based on the likelihood. These three steps are repeated at each measurement occasion. The exact reformulation of the state-space models is specified in the appendix.

Using the Kalman filter, we derive dynamic latent factor scores in real-time as a new observation arrives. Let $\mathcal{D}_{1:t} = \{\mathbf{y}_{1i1:t}, \mathbf{y}_{2i}\}_{i=1}^N$ be the collection of available

dataset at time t , $\boldsymbol{\eta}_{\text{aug},it|t-1}^{s,s'} = \mathbb{E}(\boldsymbol{\eta}_{\text{aug},it}|S_{it} = s, S_{i,t-1} = s', \mathcal{D}_{1:t-1})$ be the conditional mean vector of intra-individual augmented latent variables, $\mathbf{P}_{\text{aug},it|t-1}^{s,s'} = \text{Cov}(\boldsymbol{\eta}_{\text{aug},it}|S_{it} = s, S_{i,t-1} = s', \mathcal{D}_{1:t-1})$ be the associated covariance matrix, $\mathbf{v}_{it}^{s,s'}$ be the conditional one-step-ahead prediciton error vector of intra-individual observed variables, and $\mathbf{F}_{1it}^{s,s'}$ the associated covariance matrix. Here, the set (s, s') represent indices of the current and previous regimes. The Kalman filer procedure consists of computing the following quantities in order:

$$\boldsymbol{\eta}_{\text{aug},it|t-1}^{s,s'} = \mathbf{B}_{1is,\text{aug}} + \mathbf{B}_{3is,\text{aug}}^* \boldsymbol{\eta}_{\text{aug},i,t-1|t-1}^{s'} \quad (10)$$

$$\mathbf{P}_{\text{aug},it|t-1}^{s,s'} = \mathbf{B}_{3is,\text{aug}}^* \mathbf{P}_{\text{aug},i,t-1|t-1}^{s'} \mathbf{B}_{3is,\text{aug}}^{*T} + \mathbf{Q}_{1s,\text{aug}} \quad (11)$$

$$\mathbf{v}_{it}^{s,s'} = \mathbf{y}_{1it} - \boldsymbol{\Lambda}_{1s,\text{aug}} \boldsymbol{\eta}_{\text{aug},it|t-1}^{s,s'} \quad (12)$$

$$\mathbf{F}_{1it}^{s,s'} = \boldsymbol{\Lambda}_{1s,\text{aug}} \mathbf{P}_{\text{aug},it|t-1}^{s,s'} \boldsymbol{\Lambda}_{1s,\text{aug}}^T + \mathbf{R}_{1s} \quad (13)$$

$$\boldsymbol{\eta}_{\text{aug},it|t}^{s,s'} = \boldsymbol{\eta}_{\text{aug},it|t-1}^{s,s'} + \mathbf{K}_{it,\text{aug}}^{s,s'} \mathbf{v}_{it}^{s,s'} \quad (14)$$

$$\mathbf{P}_{\text{aug},it|t}^{s,s'} = \mathbf{P}_{\text{aug},it|t-1}^{s,s'} - \mathbf{K}_{it,\text{aug}}^{s,s'} \boldsymbol{\Lambda}_{1s,\text{aug}} \mathbf{P}_{\text{aug},it|t-1}^{s,s'} \quad (15)$$

where $\mathbf{B}_{1is,\text{aug}}^* = \begin{bmatrix} \mathbf{b}_{1s} + \mathbf{b}_{2s} \boldsymbol{\eta}_{2i} \\ \mathbf{0} \end{bmatrix}$, $\mathbf{B}_{3is,\text{aug}} = \begin{bmatrix} \mathbf{B}_{3is} & \mathbf{I} \\ \mathbf{0} & \mathbf{I} \end{bmatrix}$, $\mathbf{Q}_{\text{aug}} = \begin{bmatrix} \mathbf{Q}_{1s} & \mathbf{0} \\ \mathbf{0} & \mathbf{0} \end{bmatrix}$, $\boldsymbol{\Lambda}_{1s,\text{aug}} = \begin{bmatrix} \boldsymbol{\Lambda}_{1s} & \mathbf{0} \end{bmatrix}$. Furthermore, $\mathbf{K}_{it,\text{aug}}^{s,s'} = \mathbf{P}_{\text{aug},it|t-1}^{s,s'} \boldsymbol{\Lambda}_{1s,\text{aug}}^T \mathbf{F}_{1it}^{s,s'}^{-1}$ is called the Kalman gain function. Equation (15) is often substituted by what's called the *Joseph form* (Bucy and Joseph, 2005) because subtracting two covariance matrices may result in a numerical error causing one of the diagonal elements to be slightly less than zero. This poses a serious issue as it violates the positive (semi-)definiteness of the covariance matrix. To circumvent this issue, the *Joseph form* update can be employed. By rearranging Equation (15), we obtain

$$\mathbf{P}_{\text{aug},it|t}^{s,s'} = (\mathbf{I} - \mathbf{K}_{it,\text{aug}}^{s,s'} \boldsymbol{\Lambda}_{1s,\text{aug}}) \mathbf{P}_{\text{aug},it|t-1}^{s,s'} (\mathbf{I} - \mathbf{K}_{it,\text{aug}}^{s,s'} \boldsymbol{\Lambda}_{1s,\text{aug}})^T + \mathbf{K}_{it,\text{aug}}^{s,s'} \mathbf{R}_{1s} (\mathbf{K}_{it,\text{aug}}^{s,s'})^T, \quad (16)$$

where \mathbf{I} represents an identity matrix (of size U_{aug}). The Kalman filter summarized in Equations (10) to (16) operates recursively for $t = 1, \dots, T$ until $\boldsymbol{\eta}_{\text{aug},it|t}^{s,s'}$ and $\mathbf{P}_{\text{aug},it|t}^{s,s'}$ have been computed for all time points.

The dynamic latent factor scores at $t = 0$ is assumed to be normally distributed, i.e., $\boldsymbol{\eta}_{\text{aug},0} \sim \mathcal{N}(\boldsymbol{\eta}_{\text{aug},0|0}, \mathbf{P}_{\text{aug},0|0})$. Typically, $\boldsymbol{\eta}_{\text{aug},0}$ is assumed to have a *diffuse* density, implying that $\boldsymbol{\eta}_{\text{aug},0|0}$ is fixed to a vector of constants (e.g., a vector of zeros) and the diagonal elements of the covariance matrix $\mathbf{P}_{\text{aug},0|0}$ are set to arbitrarily large constants. However, in this R code's implementation, $\boldsymbol{\eta}_{\text{aug},0|0}$ is fixed to a zero vector,

and $\mathbf{P}_{\text{aug},0|0}$ is set to a specific block matrix $\begin{bmatrix} \mathbf{I} & \mathbf{0} \\ \mathbf{0} & \mathbf{Q}_2 \end{bmatrix}$. This reflects a more specific prior condition reflecting the prior variance of the random intercepts ζ_2 .

The extended Hamilton filter (step 3)

The Hamilton filter (Hamilton, 1989) is an algorithm to make inference in the Markov-switching model. Unlike the Kalman filter, the algorithm is specialized for the inference of discrete latent states and works as a nonlinear filter. The filter also utilizes the maximum likelihood estimation which serves as a basis for parameter optimization. Similar to the Kalman filter, the Hamilton filter consists of a *prediction* and an *update* step.

In step 3.1, the model probabilities are predicted using the transition probabilities. In step 3.2, the prediction is updated based on the new observations. The model probabilities are then reweighted by the likelihood.

Our version is an extension to the original Hamilton filter (Hamilton, 1989), accounting for within- and between-individual differences in the regime-switching trajectory. We call it the extended Hamilton filter and the recursive process can be described as

$$Pr[S_{it} = s, S_{i,t-1} = s' | \mathcal{D}_{1:t-1}] = Pr[S_{it} = s | S_{i,t-1} = s'] Pr[S_{i,t-1} = s' | \mathcal{D}_{1:t-1}], \quad (17)$$

$$f(\mathbf{y}_{1it} | \mathcal{D}_{1:t-1}) = \sum_{s,s'} f(\mathbf{y}_{1it} | S_{it} = s, S_{i,t-1} = s', \mathcal{D}_{1:t-1}) Pr[S_{it} = s, S_{i,t-1} = s' | \mathcal{D}_{1:t-1}] \quad (18)$$

$$Pr[S_{it} = s, S_{i,t-1} = s' | \mathcal{D}_{1:t}] = \frac{f(\mathbf{y}_{1it} | S_{it} = s, S_{i,t-1} = s', \mathcal{D}_{1:t-1}) Pr[S_{it} = s, S_{i,t-1} = s' | \mathcal{D}_{1:t-1}]}{f(\mathbf{y}_{1it} | \mathcal{D}_{1:t-1})} \quad (19)$$

$$Pr[S_{it} = s | \mathcal{D}_{1:t}] = \sum_{s'} Pr[S_{it} = s, S_{i,t-1} = s' | \mathcal{D}_{1:t}], \quad (20)$$

where the conditional multivariate normal likelihood function $f(\mathbf{y}_{1it} | S_{it} = s, S_{i,t-1} = s', \mathcal{D}_{1:t-1})$ is computed as

$$f(\mathbf{y}_{1it} | S_{it} = s, S_{i,t-1} = s', \mathcal{D}_{1:t-1}) = (2\pi)^{-\frac{O_1}{2}} |\mathbf{F}_{1it}^{s,s'}|^{-\frac{1}{2}} \exp \left\{ -\frac{1}{2} (\mathbf{v}_{it}^{s,s'})^T [\mathbf{F}_{1it}^{s,s'}]^{-1} \mathbf{v}_{it}^{s,s'} \right\}. \quad (21)$$

$f(\mathbf{y}_{1it} | \mathcal{D}_{1:t-1})$ in Equation (18) is called the *prediction error decomposition function* (Schweppe, 1965). The transition probabilities $Pr[S_{it} = s | S_{i,t-1} = s']$ are expressed in the same way as Equation (6). Compared with A.3 in Chow and Zhang (2013), our framework has greater flexibility because we allowed the heterogeneous transition

probabilities depending on the intra-individual latent factor scores, inter-individual latent factor scores, and their interactions.

The collapsing process (step 4)

The approximation is based on collapsing the joint estimates $\boldsymbol{\eta}_{\text{aug},it|t}^{s,s'}$ and $\mathbf{P}_{\text{aug},it|t}^{s,s'}$ at the end of each occasion into marginal estimates $\boldsymbol{\eta}_{\text{aug},it|t}^s$ and $\mathbf{P}_{\text{aug},it|t}^s$. At each time point t , the extended Kalman filter procedures utilize only the marginal estimates: $\boldsymbol{\eta}_{\text{aug},i,t-1|t-1}^{s'}$ and $\mathbf{P}_{\text{aug},i,t-1|t-1}^{s'}$, from the previous time point. Without this procedure, computational costs would be enormous due to the necessity of executing Equations (10) and (11) for 2^T combinations and storing all those results. To circumvent the issue, Kim and Nelson (2017) proposed collapsing $\boldsymbol{\eta}_{1it|t-1}^{s,s'}$ and $\mathbf{P}_{1it|t-1}^{s,s'}$ as follows:

$$\boldsymbol{\eta}_{\text{arg},it|t}^s = \sum_{s'} W_{it}^{s,s'} \boldsymbol{\eta}_{\text{arg},it|t}^{s,s'}, \quad (22)$$

$$\mathbf{P}_{\text{arg},it|t}^s = \sum_{s'} W_{it}^{s,s'} \left[\mathbf{P}_{\text{arg},t|t}^{s,s'} + (\boldsymbol{\eta}_{\text{arg},it|t}^s - \boldsymbol{\eta}_{\text{arg},it|t}^{s,s'}) (\boldsymbol{\eta}_{\text{arg},it|t}^s - \boldsymbol{\eta}_{\text{arg},it|t}^{s,s'})^T \right], \quad (23)$$

$$W_{it}^{s,s'} = \frac{Pr[S_{it} = s, S_{i,t-1} = s' | \mathcal{D}_{1:t}]}{Pr[S_{it} = s | \mathcal{D}_{1:t}]} \quad (24)$$

Here, $W_{it}^{s,s'}$ is referred to as the weighting factor. The computation of the weighting factor makes use of $Pr[S_{it} = s, S_{i,t-1} = s' | \mathcal{D}_{1:t}]$ and $Pr[S_{it} = s | \mathcal{D}_{1:t}]$ which are calculated in Equations (17) to (19).

Parameter update (step 5)

To obtain the (log-)total likelihood function $\log f(\mathbf{Y}_1 | \boldsymbol{\theta})$, we sum up the log of prediction error decomposition function over time and across persons:

$$\log f(\mathbf{Y}_1 | \boldsymbol{\theta}) = \sum_i \sum_t \log f(\mathbf{y}_{1it} | \mathcal{D}_{1:t-1}). \quad (25)$$

We then adapt the parameters based on the optimizer of choice. The convergence criteria is also based on the total likelihood function. Let $\hat{\boldsymbol{\theta}}_k$ be the parameter estimate at k th iteration step, improvement of the total likelihood is calculated as

$$\Delta \log f(\mathbf{Y}_1 | \hat{\boldsymbol{\theta}}_k) = \log f(\mathbf{Y}_1 | \hat{\boldsymbol{\theta}}_k) - \log f(\mathbf{Y}_1 | \hat{\boldsymbol{\theta}}_{k-1}) \quad (26)$$

which serves as the basis of convergence.

Point estimates of all parameters $\hat{\boldsymbol{\theta}}$ can be obtained by maximizing the total log-likelihood function $\log[f(\mathbf{Y}_1 | \boldsymbol{\theta})]$. The corresponding standard errors are obtained by taking the square root of the diagonal elements of the negative numerical Hessian

matrix at the convergence point $\mathbf{I}(\hat{\boldsymbol{\theta}})$, or its approximation using the outer product of the gradient (OPG). Let $g_i(\boldsymbol{\theta}) = \frac{\partial}{\partial \boldsymbol{\theta}} \sum_t \log f(\mathbf{y}_{1it} | \mathcal{D}_{1:t-1})$,

$$\mathbf{I}_{\text{OPG}}(\boldsymbol{\theta}) = \sum_{i=1}^N g_i(\boldsymbol{\theta}) g_i(\boldsymbol{\theta})^T. \quad (27)$$

The information matrix equality $\mathbf{I}(\boldsymbol{\theta}) = \mathbf{I}_{\text{OPG}}(\boldsymbol{\theta})$ holds given a correctly specified model and standard regularity assumptions (see White, 1982).

Missing values

Missing values often occur in ILD in psychology. Harvey (1990) successfully accommodated missing values in the Kalman filter without regime switching. When the time-dependent observed variables \mathbf{y}_{1it} contain missing values, the one-step-ahead prediction error in step 2.2 cannot be calculated. The consequences are that the likelihood function cannot be obtained and the updated estimates in step 2.3 cannot be determined. As a result, updated estimates are replaced by predicted estimates. This also applies for the extended Kalman filter.

In the case of our extended Kim filter, missing values not only affect the extended Kalman filter, but also the extended Hamilton filter. To overcome this additional issue, one can use the method proposed by Hamaker and Grasman (2012). At each time point, step 2.2 and 2.3 of the extended Kalman filter (Equation 12 to 16), the step 3.2 of the extended Hamilton filter (Equation 18 to 20), and the likelihood calculation (Equation 21) will be skipped for subjects with missing values. Instead, estimations in the update step $(\boldsymbol{\eta}_{\text{aug},it|t}^{s,s'}, \mathbf{P}_{\text{aug},it|t}^{s,s'}, \Pr[S_{it} = s, S_{i,t-1} = s' | \mathcal{D}_{1:t}])$ are substituted by the estimations in the prediction step $(\boldsymbol{\eta}_{\text{aug},it|t-1}^{s,s'}, \mathbf{P}_{\text{aug},it|t-1}^{s,s'}, \Pr[S_{it} = s, S_{i,t-1} = s' | \mathcal{D}_{1:t-1}])$.

Empirical Study

As an empirical example, we used ILD from a student dropout study in math (Kelava et al., 2022). The dataset contains three types of information: a questionnaire on the inter-individual differences, a short online survey on intra-individual differences collected over 50 time points, and attendance information for the accompanying tutorial sessions. Our sample contains 119 mathematic students at a German university. 7 intra-individual latent factors (*content not important, cost, afraid to fail, no understanding, stress, no positive affect, negative affect*) are estimated from 17 observed variables, and 1 inter-individual latent factor (*cognitive*

skills) is estimated from 2 items². Table 1 briefly summarizes the meaning of the intra- and inter-individual factors.

In the dataset, 14 individuals (11.8%) dropped out by the middle time point ($t = 25$) and 45 individuals (37.8%) dropped out by the final time point ($t = 50$). The intra-individual variables (\mathbf{y}_1) had a large proportion of missing values. Among 119×50 observations, 55.8% of the entries had at least one variable missing before the dropout and 88.2% after the dropout.

TABLE 1.

Latent factors considered in the empirical study and their corresponding observed variables used for measurement.

Factor	Item Description
Content not important (3 items)	Low attainment/utility value.
Cost (2 items)	Perceived cost of studying.
Afraid to fail (2 items)	Fear of failure and thoughts of dropping out.
Not understanding (2 items)	Lack of understanding of course content and tasks.
Stress (2 items)	Stress and being overwhelmed by the course demands.
Positive affect (3 items)	PANAS positive scale (reversed).
Negative affect (3 items)	PANAS negative scale.
Cognitive skills (2 items)	Mathematics grade from high school (Abitur). Sum score of TIMSS mathematics items.

Forecast implementation

Prior to the parameter estimation, eight assumptions are made. First, large fixed intercepts are assumed in the second regime (i.e., $\mathbf{b}_{1s} < \mathbf{b}_{12}$). This is provided so that the second latent state can be considered to be related to an intention to dropout (same assumption is made in Kelava et al., 2022). Second, in addition to model identification constraints, factor loadings ($\mathbf{A}_{1s}, \mathbf{A}_2$) are assumed to be class-invariant and sparse with no cross-loadings, in order to ensure measurement invariance (MI). Third, within- and between-level residual covariance matrix in the measurement model ($\mathbf{R}_{1s}, \mathbf{R}_2$) and the structural model ($\mathbf{Q}_{1s}, \mathbf{Q}_2$) are assumed to be diagonal and class-invariant in order to assume local independence and reduce model complexity. Fourth, conditional within-individual VAR(1) matrix (\mathbf{B}_{3s}) and matrix the conditional interaction effects (\mathbf{B}_{4s}) are assumed to be diagonal for sparsity and

²3 items were used in the original study (Kelava et al., 2022); however, one of the items had a weak correlation with others and were not useful; thus it was omitted from the analysis.

simplicity (AR(1) model is used; cf., Footnote 2 of Kelava et al., 2022). Fifth, (transition) probability to return to $S_{it} = 1$ after an $S_{i,t-1} = 2$ was set to a small value P_{12} with a small value (10^{-12}) for all individuals i and time t for model simplicity and interpretation (see Equation 6). Similar assumption was also made in the original study (Kelava et al., 2022) where a uniform prior $P_{12} \sim \text{unif}(0, 0.1)$ was used. Sixth, intercept term (γ_1) of the Markov-switching model was fixed to $\text{logit}(0.99) \approx 4.60$ for the identification of regimes, reflecting our knowledge that approximately 40% of students dropout eventually (i.e., $0.99^{50} \approx 61\%$). Seventh, interaction effects (γ_4) in the Markov-switching model are restricted to zero with respect to motivational variables (*content not important, not understanding, positive affect, negative affect*; cf., Kelava et al., 2022)³. Eighth, if a dropout is observed for a student i at time t , the regime S_{it} becomes an observed value i.e., $S_{it}, \dots, S_{iT} = 2$. This condition is to identify the second regime as *an intention to dropout*.

The estimation procedure was implemented in R (R Core Team, 2024). The model estimation and forecasting were implemented according to Algorithm 1. Our parameter optimization used Rprop (Riedmiller and Braun, 1993) with hyperparameters ($\Delta_0 = 0.01$, $\eta = (\eta_+, \eta_-) = (0.5, 1.2)$, $(\Delta_{\min}, \Delta_{\max}) = (10^{-6}, 50)$) using 3 initializations. If $\Delta \log f(\mathbf{Y}_1 | \Theta_k) < 10^{-4}$ continues 20 steps in a row, the optimization is terminated (see Equation 26). The first half of the measurements was used to estimate the parameters, and the second half was used to evaluate the out-of-sample forecasting performance.

The computations were conducted on a computer using one core of an AMD Ryzen Threadripper 3960X with 128 GB of RAM. The computation took approximately two hours.

Forecasting results

Markov-switching parameters

Parameter estimates are found in Table 3. The main between effect (γ_2) was positive. The main intra-individual effect (γ_3) was negative for 6 out of 7 parameters. The interaction effect γ_4 were negative in 2 out of 3 parameters. Large standard errors in the Markov-switching parameters require cautions. That being said, preliminary interpretations can be made by focusing on relatively large effects:

- *Cognitive skills*: For a student with average intra-individual factor scores, higher

³In other words, interaction effects are allowed only with respect to self-regulatory variables (*cost, afraid to fail, stress*). This encodes the hypothesis that cognitive measures moderate the impacts of self-regulatory aspects on dropout intention.

cognitive skills are related to *intention to dropout* and vice versa.

- *Content not important*: For a student with average cognitive skills, feeling that the content is not important is related to *intention to dropout*.
- *Cost*: For a student with average cognitive skills, cost awareness is related to *intention to dropout*. However, the higher the cognitive skills, cost awareness is related to *no intention to dropout* and vice versa.
- *Afraid to fail*: For a student with average cognitive skills, fear of failure is related to *intention to dropout*. The higher the cognitive skills, the relationship strengthens and vice versa.

Structural model parameters

No intention to dropout ($s = 1$). Parameter estimates are found in Table 4. The baseline effect (\mathbf{B}_{21}) of *cognitive skills* on the intercept was negative for all 7 within-scales. This means, persons with higher cognitive skills had lower scores on the within-scales such as *cost*. The autoregressive coefficients (diagonal elements of \mathbf{B}_{31}) were positive and large (0.88 to 0.94) for all 7 within-scales, implying that the emotional state is strongly dependent on the previous state. There are also some interactions between the within-scales and the cognitive skills.

Intention to dropout ($s = 2$). Parameter estimates are found in Table 5. Like the first state, the baseline effect (\mathbf{B}_{22}) of *cognitive skills* on the intercept was negative for all 7 within-scales. The baseline effect was not much different from the first state. The autoregressive coefficients (diagonal elements of \mathbf{B}_{32}) were also positive and large (0.88 to 0.96) for all 7 within-scales. They were larger than the first state except for *cost* and *positive affect*, implying a stronger temporal dependencies in affective state is associated with the dropout risk.

Variance estimation

Parameter estimates are found in Table 6. The within-level variances (diagonal elements of \mathbf{Q}_1) were relatively larger for *positive affect* and *negative affect*, implying a larger variation. The between level variances (diagonal elements of \mathbf{Q}_2) were predicted to be zero, implying the the inter-individual difference could be sufficiently explained by the difference in the baseline cognitive skills.

Regime probabilities

Compared with the 45 persons (37.8%) who had actually dropped out, the model predicted 76 individuals (63.9%) were predicted to have formed an intention to dropout at the middle time point ($t = 25$) and 95 individuals (79.8%) at the final

time point ($t = 50$). Among the 45 dropouts, 36 persons (80.0%) were successfully predicted to have an intention to dropout before the dropout. The average time point to switch from $s = 1$ (no intention to quit) to $s = 2$ (intention to quit) was at $t = 13.6$ ($SD = 11.8$). For the actual dropouts, this switch occurred on average at $t = 11.2$ ($SD = 10.9$) which was much earlier than the actual dropouts (on average at $t = 37.4$ ($SD = 16.1$)). The significant gap suggests early signals of dropout intentions when interventions should be conducted.

Figure 1 illustrates the trajectories of the regime probabilities corresponding to *intention to dropout* for 3 individuals compared with their actual dropout status. The left panel shows that student (#1) signaled an intention to dropout immediately and eventually dropped out. The middle panel shows that student (#15) weakly signaled an intention to dropout towards the end but did not dropout. The right panel shows that student (#31) signaled no intention to dropout and did not dropout.

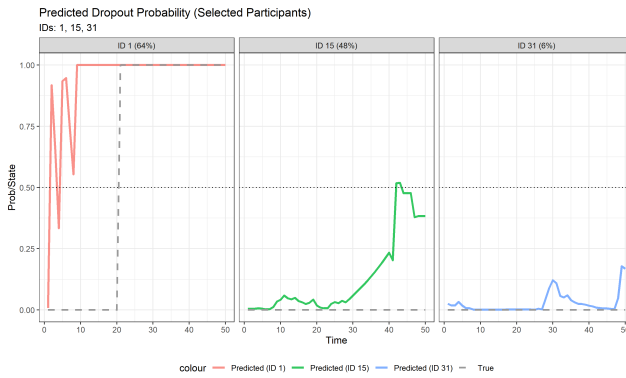


FIGURE 1.

Comparison of predicted regime probability (marginalized) and true dropout occurrence for selected individuals. The solid lines represent predicted values, while the dashed line represents true values. The dotted line at $y = 0.5$ serves as a cutoff point.

Intra-individual latent factor scores

Figure 2 illustrates dynamic trajectories of intra-individual latent factor scores. A student who dropped out (#1) exhibited consistently higher scores in *cost*, *afraid to fail*, *stress*, and *negative affect* than those remained in the program (#15, #31). Trajectories of student (#1) show a sudden increase around $t = 10$, which coincides with the timing of forming *an intention to dropout* (see Figure 1 for comparison).

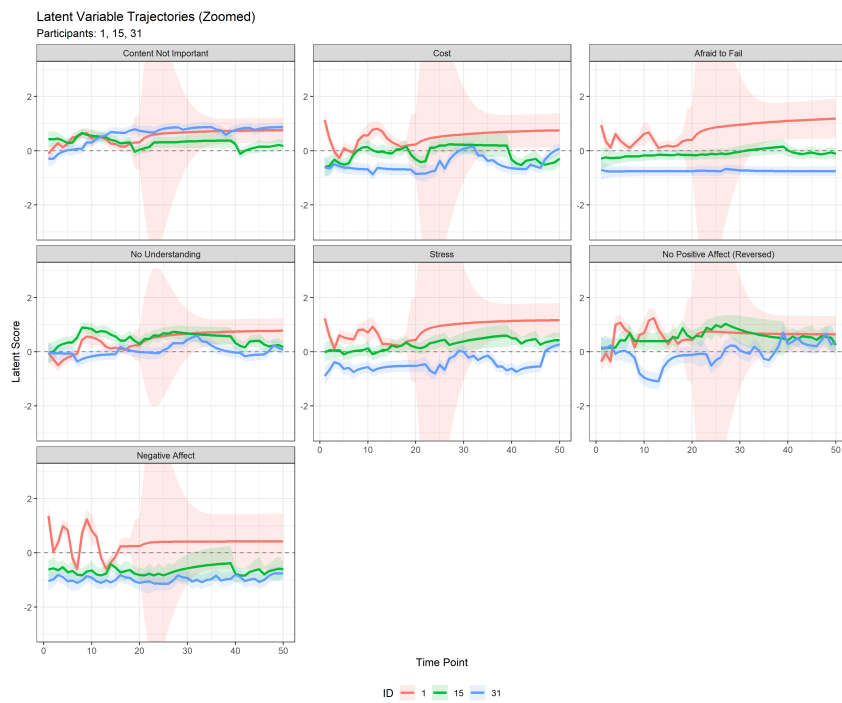


FIGURE 2.

Comparison of Factor Scores for Selected Individuals. Each panel represents a unique factor. The solid colored lines indicate factor scores for each individual, while the shaded regions represent variance bands (± 1 standard deviation).

Simulation Studies

In this section, we present a simulation study that investigates the performance of the proposed approach given complete datasets. Regime prediction, prediction of the dynamic latent variables, and parameter retrieval are evaluated with a population model that is build upon the characteristics of the empirical example in the previous section.

Data generating process

Data were generated based on the parameter estimates from the empirical study. In the simulation, however, we used only 2 dynamic latent factors (*cost*, *afraid to fail*). This reduced model complexity was necessary to keep computation time feasible for a simulation study. The first datasets (\mathcal{D}_{75}) consist of $N = 75$ individuals and $T = 50$ time points, and the second datasets (\mathcal{D}_{100}) consist of $N = 100$ individuals and $T = 50$ time points. The simulation was replicated $R = 100$ times for each data size.

Forecast implementation and evaluation

The estimation procedure was implemented in R (R Core Team, 2024). The model estimation and forecasting were implemented according to Algorithm 1. Our parameter optimization used Rprop (Riedmiller and Braun, 1993) with hyperparameters ($\Delta_0 = 0.1$, $\boldsymbol{\eta} = (\eta_+, \eta_-) = (0.5, 1.2)$, $(\Delta_{\min}, \Delta_{\max}) = (10^{-6}, 50)$) using 3 initializations. If $\Delta \log f(\mathbf{Y}_1 | \Theta_k) < 10^{-4}$ continues 20 steps in a row, the optimization is terminated (see Equation 26). The first half of the measurements was used to estimate the parameters, and the second half was used to evaluate the out-of-sample forecasting performance.

For evaluation, First, we investigated the *accuracy*, *sensitivity* and *specificity* for the prediction of the underlying regime memberships. We distinguished the performance within the observed data ($t = 1, \dots, 25$) and the forecast data ($t = 26, \dots, 50$). Second, a score function is used to evaluate the forecast of the dynamic latent factors by

$$\delta_t = \frac{1}{N} \sum_i \sum_j (\hat{\eta}_{itj} - \eta_{itj})^2, \quad i = 1, \dots, N, \quad j = 1, 2 \quad (28)$$

for each forecast time point $t = 26, \dots, 50$ (cf., Gneiting, 2011). Third, our parameter estimation was evaluated in terms of the bias compared to the true values, standard deviation of estimates across replications, and RMSE.

Forecasting results

Parameter estimation Table 10 and 11 summarizes the results (see appendix). Speaking of structural and measurement model parameters, bias, SD, RMSE were smaller for a larger sample size (\mathcal{D}_{100} compared with \mathcal{D}_{75}). For Markov-switching parameters, parameter estimates for \mathcal{D}_{100} was not better than \mathcal{D}_{75} .

Regime membership Table 2 summarizes the performance of regime-switching predictions. Accuracy for the regime prediction was around 80% for both data sizes. This indicates that the regime-switches were consistently detected, regardless of the sample size. In both datasets, relatively high specificity (84 ~ 91% compared with 62 ~ 67% for sensitivity) was observed. All three metrics slightly improved for a larger sample size (\mathcal{D}_{100}) in the forecast interval.

TABLE 2.
Sensitivity and specificity for the regime prediction.

Data	Accuracy		Sensitivity		Specificity	
	Observed	Forecast	Observed	Forecast	Observed	Forecast
\mathcal{D}_{75}	0.80	0.79	0.62	0.71	0.91	0.84
\mathcal{D}_{100}	0.81	0.80	0.63	0.72	0.90	0.87

Dynamic latent variables The (quadratic) score function shows the average Euclidean distance between the actual factor scores and the forecast ones. The score indicates the precision of the forecast for each forecast time point. Figure 3 indicates that a large sample size (\mathcal{D}_{100}) resulted in a consistently lower score function and a smaller standard deviation compared with a small sample size (\mathcal{D}_{75}) throughout the forecast interval.

Discussion

Many psychological change processes are characterized by discontinuous state transitions. The flexibility of RSSS modeling framework allows researchers to include interactions between the intra-individual and inter-individual level. This is often necessary in order to validly represent the dynamic underlying processes (e.g., where baseline covariates modulate how current affective states impact decisions). We presented a frequentist approach to estimating such flexible RSSS models. The development of the estimation procedure enables forecasting and inferences in real-time.

The extended Kim filter proposed here, serves as an effective tool for detecting unobserved change processes or regime-switches. The effectiveness is particu-

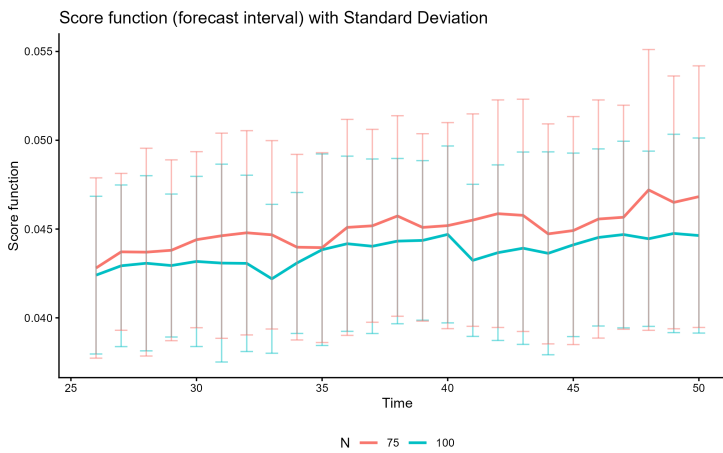


FIGURE 3.

Score function under the different conditions of sample size across the forecast time points.

larly utilized when such changes manifest through variations at the within- and between-levels in each individual. The described model and estimation procedures can accommodate a wide variety of dynamic models.

Our model can be readily extended to accommodate three or more regimes, or a more flexible state-space representation, such as incorporating a higher order autoregression, within-between interaction effects, or a polynomial function (cf. Chow and Zhang, 2013). Another interesting extension is to extend the Markov-switching models: incorporating higher-order autoregressive terms and their interactions, or using polynomial functions, will make the model transition mechanism more flexible.

Open questions

This article did not evaluate the performance under different degree of missingness. Our empirical and simulation study presented two extremes: one with a large proportion of missingness and the other with a complete dataset. The missing proportion in our empirical dataset had a big gap before and after the dropout, clear indication that the the data not even made missing completely at random (MCAR).

Our classification result is dependent on the proportion of clusters. Basically, in the case of imbalanced data, as observed in our simulation studies, it would be more difficult to identify the classes which have smaller sample sizes. Furthermore, due to the nature of clustering algorithms, the performance of our method might be sensitive to the similarities of regime distributions. If the regime distributions are very similar (i.e., distribution with large overlapping), the performance is expected to deteriorate.

Direct comparison with Bayesian counterpart (Kelava et al., 2022) would be an interesting future direction. In order to make a full comparison, all the Bayesian priors need to be substituted by uninformative ones. Bayesian inference with informative prior is a regularized estimation and will not be equivalent to our fully data-driven frequentist framework. Changing all the informative priors to uninformative ones is expected to be time-consuming due to the curse of dimensionality, given that the current Bayesian implementation already requires a lot of time to compute.

Lastly, identifying the correct model is not trivial in practice, as any model is an approximation in social science (Browne and Cudeck, 1992). Model estimation using a misspecified model is known to harm the prediction in SEM (de Rooij et al., 2023). In longitudinal models, structural misspecification can be found in many parts including measurement model (e.g., omitting lagged cross-loadings), time-series model (e.g., choosing wrong order in VAR), and model heterogeneity (e.g., ignoring within-person model switch). Under model uncertainty, model stacking approaches (e.g., Yao et al., 2022) may offer an alternative solution by accommodating many ($\gg 2$) models/regimes in a flexible manner. The average sensitivity was much greater than the specificity, which is the direct result of a high percentage of 2nd regime proportions i.e., highly unbalanced data.

Data Availability The associated replication files for the simulation study, including all analysis code, are available online at <https://github.com/PsychometricsMZ/Regime-switching>. The empirical data used for the application study cannot be made publicly available due to the terms of the data disclosure agreement and privacy concerns.

References

Anja Achtziger and Peter M. Gollwitzer. *Motivation and Volition in the Course of Action*, pages 485–527. Springer International Publishing, Cham, 2018. ISBN 978-3-319-65094-4. doi: 10.1007/978-3-319-65094-4_12. URL https://doi.org/10.1007/978-3-319-65094-4_12.

Tihomir Asparouhov, Ellen L. Hamaker, and Bengt Muthén. Dynamic latent class analysis. *Structural Equation Modeling: A Multidisciplinary Journal*, 24(2):257–269, 2017. doi: 10.1080/10705511.2016.1253479.

M. S. Bartlett. The statistical conception of mental factors. *British Journal of Psychology. General Section*, 28(1):97–104, 1937. doi: <https://doi.org/10.1111/j.2044-8295.1937.tb00863.x>.

G.E.P. Box, G.M. Jenkins, G.C. Reinsel, and G.M. Ljung. *Time Series Analysis: Forecasting and Control*. Wiley Series in Probability and Statistics. Wiley, 2015. ISBN 9781118674925. URL <https://books.google.de/books?id=rNt5CgAAQBAJ>.

Michael W. Browne and Robert A. Cudeck. Alternative ways of assessing model fit. *Sociological Methods & Research*, 21:230 – 258, 1992. URL <https://api.semanticscholar.org/CorpusID:120166447>.

R.S. Bucy and P.D. Joseph. *Filtering for Stochastic Processes with Applications to Guidance*. AMS Chelsea Publishing Series. AMS Chelsea Pub., 2005. ISBN 9780821837825. URL <https://books.google.de/books?id=RnEHZA0M61cC>.

Sy Miin Chow and Guangjian Zhang. Nonlinear regime-switching state-space (rsss) models. *Psychometrika*, 78(4):740–768, October 2013. ISSN 0033-3123. doi: 10.1007/s11336-013-9330-8.

Mark de Rooij, Julian D. Karch, Marjolein Fokkema, Zsuzsa Bakk, Bunga Citra Pratiwi, and Henk Kelderman. Sem-based out-of-sample predictions. *Structural Equation Modeling: A Multidisciplinary Journal*, 30(1):132–148, 2023. doi: 10.1080/10705511.2022.2061494. URL <https://doi.org/10.1080/10705511.2022.2061494>.

Tilmann Gneiting. Making and evaluating point forecasts. *Journal of the American Statistical Association*, 106(494):746–762, 2011. doi: 10.1198/jasa.2011.r10138.

E.L. Hamaker and R.P.P.P. Grasman. Regime switching state-space model applied to psychological processes: Handling missing data and making inferences. *Psychometrika*, 77:400–422, 2012. ISSN 0033-3123.

James D. Hamilton. A new approach to the economic analysis of nonstationary time series and the business cycle. *Econometrica*, 57(2):357–384, 1989. ISSN 00129682, 14680262. URL <http://www.jstor.org/stable/1912559>.

A.C. Harvey. *Forecasting, Structural Time Series Models and the Kalman Filter*. Cambridge University Press, 1990. ISBN 9780521405737. URL <https://books.google.de/books?id=Kc6tnRHBwLcC>.

Linying Ji, Sy-Miin Chow, Brian Crosby, and Douglas M. Teti. Exploring sleep dynamic of mother-infant dyads using a regime-switching vector autoregressive model. *Multivariate Behavioral Research*, 55(1):150–151, 2020. doi: 10.1080/00273171.2019.1697863.

R. E. Kalman. A New Approach to Linear Filtering and Prediction Problems.

Journal of Basic Engineering, 82(1):35–45, 03 1960. ISSN 0021-9223. doi: 10.1115/1.3662552.

Augustin Kelava and Holger Brandt. A nonlinear dynamic latent class structural equation model. *Structural Equation Modeling: A Multidisciplinary Journal*, 26(4):509–528, 2019. doi: 10.1080/10705511.2018.1555692.

Augustin Kelava, Pascal Kilian, Judith Glaesser, Samuel Merk, and Holger Brandt. Forecasting Intra-individual Changes of Affective States Taking into Account Inter-individual Differences Using Intensive Longitudinal Data from a University Student Dropout Study in Math. *Psychometrika*, 87(2):533–558, June 2022. doi: 10.1007/s11336-022-09858-.

Chang-Jin Kim. Dynamic linear models with markov-switching. *Journal of Econometrics*, 60(1):1–22, 1994. ISSN 0304-4076. doi: [https://doi.org/10.1016/0304-4076\(94\)90036-1](https://doi.org/10.1016/0304-4076(94)90036-1).

C.J. Kim and C.R. Nelson. *State-Space Models with Regime Switching: Classical and Gibbs-Sampling Approaches with Applications*. MIT Press, 2017. ISBN 9780262535502. URL <https://books.google.de/books?id=1tB3swEACAAJ>.

R Core Team. *R: A Language and Environment for Statistical Computing*. R Foundation for Statistical Computing, Vienna, Austria, 2024. URL <https://www.R-project.org/>.

M. Riedmiller and H. Braun. A direct adaptive method for faster backpropagation learning: the rprop algorithm. In *IEEE International Conference on Neural Networks*, pages 586–591 vol.1, 1993. doi: 10.1109/ICNN.1993.298623.

F. Schweppe. Evaluation of likelihood functions for gaussian signals. *IEEE Transactions on Information Theory*, 11(1):61–70, 1965. doi: 10.1109/TIT.1965.1053737.

Anders Skrondal and Petter Laake. Regression among factor scores. *Psychometrika*, 66(4):563–575, December 2001. doi: 10.1007/BF02296196. URL <https://ideas.repec.org/a/spr/psycho/v66y2001i4p563-575.html>.

Ellen L. Hamaker Tihomir Asparouhov and Bengt Muthén. Dynamic structural equation models. *Structural Equation Modeling: A Multidisciplinary Journal*, 25(3):359–388, 2018. doi: 10.1080/10705511.2017.1406803.

Timothy J. Trull and Ulrich Ebner-Priemer. The role of ambulatory assessment in psychological science. *Current Directions in Psychological Science*, 23(6):466–470, 2014. doi: 10.1177/0963721414550706.

M. West and J. Harrison. *Bayesian Forecasting and Dynamic Models*. Springer

Series in Statistics. Springer New York, 2006. ISBN 9780387227771. URL <https://books.google.de/books?id=0mPgBwAAQBAJ>.

Halbert White. Maximum likelihood estimation of misspecified models. *Econometrica*, 50(1):1–25, 1982. ISSN 00129682, 14680262. URL <http://www.jstor.org/stable/1912526>.

Manshu Yang and Sy-Miin Chow. Using state-space model with regime switching to represent the dynamics of facial electromyography (emg) data. *Psychometrika*, 75(4):744–771, 2010. doi: 10.1007/s11336-010-9176-2.

Yuling Yao, Gregor Pirš, Aki Vehtari, and Andrew Gelman. Bayesian hierarchical stacking: Some models are (somewhere) useful. *Bayesian Analysis*, 17(4), December 2022. ISSN 1936-0975. doi: 10.1214/21-ba1287. URL <http://dx.doi.org/10.1214/21-BA1287>.

Appendix

Augmented State-Space Formulation

To apply the extended Kim filter, the model defined by Equations (1), (3), and (4) is rewritten into an augmented state-space form. This augmentation combines the $U_1 \times 1$ time-dependent state $\boldsymbol{\eta}_{1it}$ and the $U_1 \times 1$ time-invariant random intercept residual ζ_{2i} into a single $U_{\text{aug}} \times 1$ state vector (where $U_{\text{aug}} = 2U_1$):

$$\boldsymbol{\eta}_{\text{aug},it} = \begin{bmatrix} \boldsymbol{\eta}_{1it} \\ \zeta_{2i} \end{bmatrix} \quad (29)$$

The parameters for the augmented Kalman filter (Equations 10 - 16) are defined by mapping this augmented state to the original model equations.

Augmented within-level measurement model

The measurement model (Equation 1) is expressed using this augmented state:

$$\mathbf{y}_{1it} = \begin{bmatrix} \mathbf{\Lambda}_{1s} & \mathbf{0} \end{bmatrix} \begin{bmatrix} \boldsymbol{\eta}_{1it} \\ \zeta_{2i} \end{bmatrix} + \boldsymbol{\epsilon}_{1it} = \mathbf{\Lambda}_{1s,\text{aug}} \boldsymbol{\eta}_{\text{aug},it} + \boldsymbol{\epsilon}_{1it} \quad (30)$$

where the augmented factor loading matrix $\mathbf{\Lambda}_{1s,\text{aug}}$ (dimensions $O_1 \times U_{\text{aug}}$) is defined as $\mathbf{\Lambda}_{1s,\text{aug}} = \begin{bmatrix} \mathbf{\Lambda}_{1s} & \mathbf{0} \end{bmatrix}$. The measurement noise covariance matrix \mathbf{R}_{1s} remains unchanged.

Augmented within-level structural model

The structural models (Equations 3 and 4) are combined to form the state transition equation. First, substituting Equation (4) into (3) yields:

$$\boldsymbol{\eta}_{1it} = (\mathbf{b}_{1s} + \mathbf{b}_{2s}\boldsymbol{\eta}_{2i}) + \mathbf{B}_{3is}\boldsymbol{\eta}_{1i,t-1} + \boldsymbol{\zeta}_{2i} + \boldsymbol{\zeta}_{1it} \quad (31)$$

The time-invariant nature of the random intercept $\boldsymbol{\zeta}_{2i}$ is defined by the identity:

$$\boldsymbol{\zeta}_{2i} = \mathbf{0} + \mathbf{0} \cdot \boldsymbol{\eta}_{1i,t-1} + \mathbf{I} \cdot \boldsymbol{\zeta}_{2i} + \mathbf{0} \quad (32)$$

Writing Equations (31) and (32) in matrix form for the augmented state $\boldsymbol{\eta}_{\text{aug},it}$ gives the state transition equation:

$$\begin{bmatrix} \boldsymbol{\eta}_{1it} \\ \boldsymbol{\zeta}_{2i} \end{bmatrix} = \begin{bmatrix} \mathbf{b}_{1s} + \mathbf{b}_{2s}\boldsymbol{\eta}_{2i} \\ \mathbf{0} \end{bmatrix} + \begin{bmatrix} \mathbf{B}_{3is} & \mathbf{I} \\ \mathbf{0} & \mathbf{I} \end{bmatrix} \begin{bmatrix} \boldsymbol{\eta}_{1i,t-1} \\ \boldsymbol{\zeta}_{2i} \end{bmatrix} + \begin{bmatrix} \boldsymbol{\zeta}_{1it} \\ \mathbf{0} \end{bmatrix} \quad (33)$$

This directly corresponds to the augmented Kalman filter's state equation (Equation 10), defining the augmented parameters as $\mathbf{B}_{1is,\text{aug}}^* = \begin{bmatrix} \mathbf{b}_{1s} + \mathbf{b}_{2s}\boldsymbol{\eta}_{2i} \\ \mathbf{0} \end{bmatrix}$ and $\mathbf{B}_{3is,\text{aug}} = \begin{bmatrix} \mathbf{B}_{3is} & \mathbf{I} \\ \mathbf{0} & \mathbf{I} \end{bmatrix}$. The augmented process noise covariance $\mathbf{Q}_{1s,\text{aug}}$ is the covariance of the residual vector $\begin{bmatrix} \boldsymbol{\zeta}_{1it} \\ \mathbf{0} \end{bmatrix}$, which is defined as $\mathbf{Q}_{1s,\text{aug}} = \begin{bmatrix} \mathbf{Q}_{1s} & \mathbf{0} \\ \mathbf{0} & \mathbf{0} \end{bmatrix}$.

TABLE 3.

Parameter estimates for the Markov-switching model. Parameter with asterisk is fixed for identification.

Parameter	Index	Estimates	SE
γ_1	1	4.60*	NA
γ_2	1	-0.93	1.72
γ_3	1	-3.92	2.82
	2	-3.28	1.91
	3	-2.58	1.91
	4	0.76	3.03
	5	-0.78	2.56
	6	-0.24	1.91
	7	-0.97	1.46
γ_4	2	1.55	4.08
	3	-2.28	5.94
	5	-1.35	4.06
P_{12}	1	10^{-12*}	NA

TABLE 4.
Parameter estimates for the structural parameters ($s = 1$).

Parameter	Index	Estimates	SE
b_{11}	1	0.04	0.02
	2	-0.01	0.02
	3	-0.01	0.02
	4	0.02	0.03
	5	0.03	0.02
	6	0.03	0.03
	7	-0.07	0.04
b_{21}	1	-0.02	0.02
	2	-0.03	0.06
	3	-0.03	0.02
	4	-0.03	0.05
	5	-0.05	0.04
	6	-0.01	0.05
	7	-0.04	0.05
$diag(\mathbf{B}_{31})$	1	0.89	0.05
	2	0.94	0.05
	3	0.93	0.03
	4	0.91	0.04
	5	0.90	0.05
	6	0.91	0.04
	7	0.88	0.05
$diag(\mathbf{B}_{41})$	1	0.05	0.08
	2	0.01	0.05
	3	0.00	0.04
	4	0.01	0.10
	5	0.00	0.06
	6	0.04	0.12
	7	0.00	0.05

TABLE 5.
Parameter estimates for the structural parameters ($s = 2$).

Parameter	Index	Estimates	SE
b_{12}	1	0.06	0.03
	2	0.06	0.06
	3	0.06	0.02
	4	0.07	0.04
	5	0.12	0.05
	6	0.09	0.04
	7	0.04	0.05
b_{22}	1	-0.02	0.05
	2	-0.02	0.09
	3	-0.03	0.03
	4	-0.04	0.06
	5	-0.04	0.09
	6	-0.01	0.07
	7	-0.01	0.06
$diag(\mathbf{B}_{32})$	1	0.93	0.05
	2	0.93	0.11
	3	0.96	0.03
	4	0.91	0.06
	5	0.91	0.06
	6	0.88	0.06
	7	0.93	0.06
$diag(\mathbf{B}_{42})$	1	0.02	0.12
	2	0.01	0.18
	3	0.02	0.03
	4	0.02	0.12
	5	0.02	0.11
	6	0.03	0.14
	7	0.00	0.08

TABLE 6.

Parameter estimates for the residual variances and $P_2 = \text{var}(\eta_{2i})$ of the structural model. Parameter with asterisk is fixed for identification.

Parameter	Index	Estimates	SE
Q_1	1	0.02	0.01
	2	0.03	0.01
	3	0.01	0.00
	4	0.02	0.00
	5	0.03	0.01
	6	0.09	0.04
	7	0.09	0.05
Q_2	1	0.00	NA
	2	0.00	NA
	3	0.00	NA
	4	0.00	NA
	5	0.00	NA
	6	0.00	NA
	7	0.00	NA
P_2	1	0.74*	NA

TABLE 7.

Parameter estimates for the factor loadings.

Parameter	Index	Estimates	SE
$\Lambda_{1,\text{free}}$	1	1.29	0.11
	2	1.03	0.08
	3	0.92	0.10
	4	0.92	0.07
	5	1.14	0.07
	6	1.09	0.08

TABLE 8.

Parameter estimates for the residual variances of the measurement model. Parameter with asterisk is fixed for identification.

Parameter	Index	Estimates	SE
R_1	1	0.37	0.04
	2	0.29	0.04
	3	0.50	0.03
	4	0.26	0.04
	5	0.29	0.04
	6	0.32	0.03
	7	0.35	0.05
	8	0.31	0.04
	9	0.36	0.05
	10	0.29	0.05
	11	0.24	0.03
	12	0.40	0.05
	13	0.53	0.07
	14	0.66	0.04
	15	0.56	0.07
	16	0.32	0.06
	17	0.49	0.08
R_2	1	0.47	39.29
	2	0.54	44.98

TABLE 9.

Summary statistics for Markov-switching model parameter estimates. Parameter with asterisk is fixed for identification.

Parameter	Index	True θ	Mean $\hat{\theta}$		Bias		RMSE		SD	
			\mathcal{D}_{75}	\mathcal{D}_{100}	\mathcal{D}_{75}	\mathcal{D}_{100}	\mathcal{D}_{75}	\mathcal{D}_{100}	\mathcal{D}_{75}	\mathcal{D}_{100}
γ_1	1	4.60	4.60*	4.60*	NA	NA	NA	NA	NA	NA
γ_2	1	-0.93	-0.03	0.02	0.91	0.96	2.00	2.69	1.79	2.53
γ_3	1	-3.28	-3.32	-3.80	-0.04	-0.52	2.92	4.08	2.93	4.06
	2	-2.58	-3.00	-3.55	-0.42	-0.97	3.41	5.13	3.40	5.06
γ_4	1	1.55	1.00	0.23	-0.55	-1.32	2.19	7.06	2.13	6.97
	2	-2.28	-1.19	-1.47	1.08	0.81	2.60	2.75	2.37	2.64
P_{12}	1	10^{-12}	$10^{-12}*_{}$	$10^{-12}*_{}$	NA	NA	NA	NA	NA	NA

TABLE 10.
Summary statistics for structural model parameter estimates.

Parameter	Index	True θ	Mean $\hat{\theta}$		Bias		RMSE		SD	
			\mathcal{D}_{75}	\mathcal{D}_{100}	\mathcal{D}_{75}	\mathcal{D}_{100}	\mathcal{D}_{75}	\mathcal{D}_{100}	\mathcal{D}_{75}	\mathcal{D}_{100}
b_{11}	1	-0.01	-0.01	-0.01	0.01	0.01	0.01	0.01	0.01	0.01
	2	-0.01	0.00	0.00	0.01	0.01	0.01	0.01	0.01	0.01
b_{12}	1	0.06	0.14	0.11	0.09	0.05	0.19	0.12	0.17	0.11
	2	0.06	0.17	0.15	0.11	0.05	0.22	0.12	0.19	0.11
b_{21}	1	-0.03	-0.02	-0.01	0.01	0.01	0.02	0.02	0.01	0.01
	2	-0.03	-0.02	-0.02	0.01	0.01	0.02	0.02	0.01	0.01
b_{22}	1	-0.02	-0.03	-0.03	-0.01	0.00	0.14	0.08	0.14	0.08
	2	-0.03	-0.03	-0.05	0.01	-0.01	0.15	0.12	0.15	0.12
$diag(\mathbf{B}_{31})$	1	0.94	0.94	0.95	0.01	0.01	0.02	0.02	0.02	0.02
	2	0.93	0.95	0.95	0.02	0.02	0.02	0.02	0.02	0.02
$diag(\mathbf{B}_{32})$	1	0.93	0.84	0.88	-0.10	-0.05	0.21	0.11	0.19	0.10
	2	0.96	0.85	0.87	-0.11	-0.09	0.21	0.19	0.18	0.17
$diag(\mathbf{B}_{41})$	1	0.01	0.00	0.01	0.00	0.00	0.01	0.01	0.01	0.01
	2	0.00	0.01	0.01	0.01	0.01	0.02	0.01	0.01	0.01
$diag(\mathbf{B}_{42})$	1	0.01	0.01	0.01	-0.01	0.00	0.08	0.07	0.08	0.07
	2	0.02	0.01	0.02	-0.01	0.00	0.11	0.08	0.11	0.08
Q_1	1	0.03	0.02	0.02	-0.01	-0.01	0.01	0.01	0.00	0.00
	2	0.01	0.01	0.01	0.00	0.00	0.01	0.01	0.00	0.00
Q_2	1	0.00	0.00	0.00	0.00	0.00	0.00	0.00	0.00	0.00
	2	0.00	0.00	0.00	0.00	0.00	0.00	0.00	0.00	0.00
P_2	1	0.74	1.04	1.04	0.29	0.30	0.37	0.34	0.22	0.15

TABLE 11.
Summary statistics for measurement model parameter estimates.

Parameter	Index	True θ	Mean $\hat{\theta}$		Bias		RMSE		SD	
			\mathcal{D}_{75}	\mathcal{D}_{100}	\mathcal{D}_{75}	\mathcal{D}_{100}	\mathcal{D}_{75}	\mathcal{D}_{100}	\mathcal{D}_{75}	\mathcal{D}_{100}
R_1	1	0.26	0.26	0.26	0.00	0.00	0.01	0.01	0.01	0.01
	2	0.29	0.28	0.29	0.00	0.00	0.01	0.01	0.01	0.01
	3	0.32	0.32	0.31	0.00	-0.01	0.01	0.01	0.01	0.01
	4	0.35	0.35	0.35	-0.01	0.00	0.01	0.01	0.01	0.01
R_2	1	0.47	1.09	0.82	0.63	0.36	2.67	2.06	2.61	2.04
	2	0.54	1.08	0.89	0.54	0.36	2.64	2.13	2.59	2.11